Available online at www.sciencedirect.com
ScienceDirect
International Journal of Thermal Sciences 46 (2007) 172–179
International Journal of Thermal Sciences
www.elsevier.com/locate/ijts

Thermodynamic bounds for food deep chilling tray tunnel operation

Maxime Ducoulombier [a], Mikhaïl Sorin [b], Alberto Teyssedou [a,*]

[a] *Engineering Physics Department, École Polytechnique, CP 6079, succ. Centre-ville, Montréal, Québec H3C 3A7, Canada*
[b] *Process Integration Section, CANMET Energy Diversification Research Laboratory, 1615 Lionel-Boulet Blvd., PO Box 4800, Varennes, Québec J3X 1S6, Canada*

Received 2 August 2005; accepted 5 May 2006

Available online 11 July 2006

Abstract

In this paper a thermodynamically guided intensification method on tray tunnels for food deep chilling is presented. Two indicators of the performance of the system are used: the exergy power and the destruction of specific exergy. The objective function corresponds to the maximization of the exergy power and the minimization of the specific exergy destruction. Exergy has the main advantage to take into consideration both the food mass flow rate and its output temperature level. The food mass flow rate stands for its quantity whereas the temperature level represents its quality. An endoreversible model is also presented in conjunction with a simple mathematical description of the refrigeration cycle internal irreversibilities. A numerical investigation against operation variables permits to find the so-called intensification zone that defines bounds for food mass flow rate and output temperature as well as for the refrigeration cycle evaporator temperature.

Keywords: Chilling tray; Food freezing; Exergy intensification; Finite-time thermodynamics

1. Introduction

The present study intends to be a follow-up of the work of Kiranoudis and Markatos [1], where a procedure is described for the optimization of a tray tunnel for meat deep chilling. In this work, the authors used an objective function based on the cost per unit of food produced. Moreover, by keeping the cold temperature level (output temperature) constant, an optimal configuration was found within a range of cooling load, i.e., a range of food mass flow rates. Whereas in their study [1], the principal goal was the maximization of a function similar to the energy efficiency, the work presented in this paper is intended to use the recent advances in finite-time thermodynamics [2–4] to intensify this kind of processes once the best operation design is known. This means that for a given system with constrained dimensions, the purpose of this work consists of finding the maximum of wanted effect, i.e., the exergy power of the cold production. As the main variable is the food outlet, there is now a tradeoff between the food quantity and the coldest temperature level it can reach. Thus, the exergy is chosen as the function to be maximized as it represents well the desired compromise between maximum food flow rate and lowest possible temperature. Taking into account that, in general, the maximum exergy does not necessarily correspond to operational needs, a region where the multi-objective optimization should be carried, must be identified.

2. The endoreversible model

The mathematical model of the chilling tunnel presented by Kiranoudis and Markatos [1], includes a simple description of the heat transfer from wide spread material slabs, i.e., beef steaks, to the refrigerant. The slabs are cooled with air under a controlled temperature (T_{CA}). The heat transfer equations take into account heat conduction in the slabs, so that a temperature profile in the material can be calculated provided that convection heat transfer stands for the boundary condition at the surface. For the sake of simplicity, they have ignored the heat transferred from the slab edges. Moreover, they have determined the thermal conductivity by using a structural model while the convection heat transfer coefficient is considered constant, independent of the air velocity.

* Corresponding author. Tel.: +1(514) 340 4711 ext. 4522; fax: +1(514) 340 4192.
E-mail address: alberto.teyssedou@polymtl.ca (A. Teyssedou).

1290-0729/$ – see front matter
doi:10.1016/j.ijthermalsci.2006.05.001

Nomenclature

A	heat exchanger surface area	m^2
AU	overall heat transfer coefficient	$W K^{-1}$
c	specific heat capacity	$J kg^{-1} K^{-1}$
$c_{apparent}$	apparent specific heat capacity of the frozen food	$J kg^{-1} K^{-1}$
$c_{unfrozen}$	specific heat capacity of the unfrozen food	$J kg^{-1} K^{-1}$
d	destruction of specific exergy	$J kg^{-1}$
D	destruction of exergy power	W
E	exergy flow rate associated with the food	W
H	enthalpy flow rate associated with the food	W
m	food mass flow rate	$kg s^{-1}$
m_R	refrigerant mass flow rate	$kg s^{-1}$
N_T	number of trucks	
P	exergy power	W
Q_E	refrigeration load	W
Q_C	heat rejected at the condenser	W
T	temperature	K
$\widetilde{T}$	entropic average temperature	K
T_{W1}	condenser inlet temperature of the water coolant	
T_{W2}	condenser outlet temperature of the water coolant	
W	power consumed by the compressor	W
W_R	work received by the refrigerant	W
x	relative position in the tunnel from the entrance to the exit	

Greek symbols

Δh_R	refrigerant specific enthalpy of evaporation	$J kg^{-1}$
η_C	isentropic efficiency of the compressor	
η_E	exergy efficiency	
θ	Carnot function	
τ_T	residence time of a truck	s

Subscripts

0	nominal operation condition
C	condenser
CA	cooling air
E	evaporator
F	fans
in	inlet of the tunnel
out	outlet of the tunnel
S	food slabs
W	water coolant

Superscripts

0	nominal operation condition

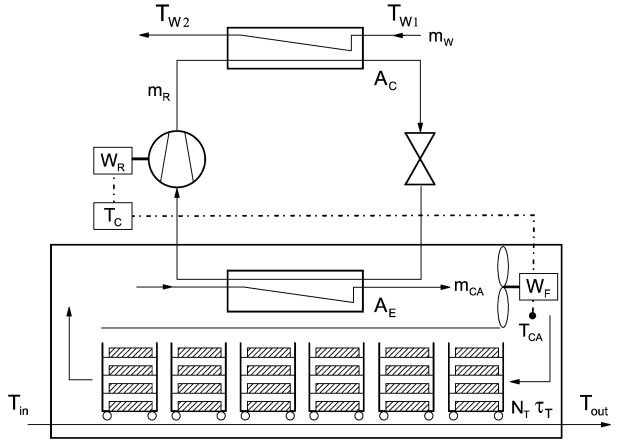

Fig. 1. Representation of industrial tray tunnels given in [1].

Fig. 1 shows a simple representation of the industrial tray tunnel given by Kiranoudis and Markatos [1]. For carrying out the optimization process, they considered the temperatures T_{in}, T_{out} and T_{W1} as constraint parameters of the process, whereas the remaining quantities were considered as optimization variables. For a given product capacity, i.e., for a given heat to be removed, the authors determined the appropriate cooling air temperature (T_{CA}), cooling air flow rate (m_{CA}), number of truck (N_T), residence time of each truck (τ_T) and number of parallel tunnels with a view to minimize the total annual cost of the system. This cost was divided into the capital cost due to the tunnel length, the number of trucks (N_T), the fan capacity (W_F), the refrigeration capacity (W_R), the heat exchangers surface areas (A_E, A_C), and the operation cost due to energy consumption of refrigeration cycle and fans, as well as the cost of cooling water consumption (m_W). All the elements of the capital cost obey the economy of scale laws.

The aim of the present work consists of using a similar representation to that given in [1] in order to deduce a simple model more appropriate for carrying out an intensification calculation. Thus, it is assumed that the system operates at nominal conditions in such a way that the fans and the cooling medium have finite maximum heat capacities. Therefore, when their energies are intensified, they do not constitute variables but constants to be added to the refrigeration energy. For instance, if the air flow rate and the number of trucks are constant then, a constant overall heat transfer coefficient between the material and the refrigerant at the evaporator (AU_E) will be considered. Note that the air, which is considered as an intermediate fluid, will not appear explicitly anymore in the present treatment. Knowing the temperature T_{CA} is equivalent to knowing the temperature of the refrigerant at the evaporator. In the same manner, for a given water flow rate, the overall heat transfer coefficient (AU_C) between the refrigerant in the condenser and the outdoor air will be considered as constant. Moreover, for exergy calculations it is quite convenient to consider that $T_{W1} = T_{\text{in}} = T_0$ ($T_0 =$ temperature of the environment). In order to further simplify the model, the cooling load is completely balanced by the heat removed from the food, i.e., the fan power does not contribute to the refrigeration load. Although actual chilling tunnels operate in a discrete manner, we represent the succession of

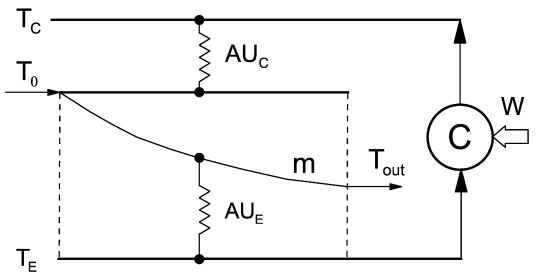

Fig. 2. Endoreversible model of a typical industrial tray tunnel.

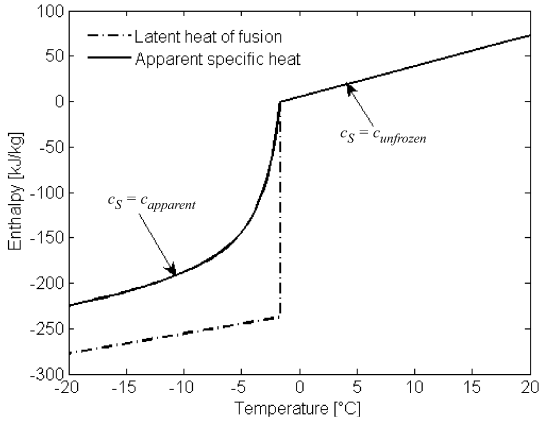

Fig. 3. Specific enthalpy as a function of temperature of meat (Beef round, full cut, lean).

material batch as a continuous flow of mass. These hypotheses allow the endoreversible model shown in Fig. 2 to be applied.

Considering that the mass flow rate (m) is the only optimization variable, then the output temperature (T_{out}) will be free to change. This is a major difference with respect to the initial optimization carried out by Kiranoudis and Markatos [1]. Although, in practice, the food output temperature is not allowed to vary outside a specified interval, our theoretical study overrides this limit. In addition, assuming that the heat conduction of the slabs is infinite, the food will have a defined temperature for a given position in the tunnel. Thus, the output temperature will be the equilibrium temperature, necessary to carry out the overall balance of energy and exergy. The effect due to heat conduction is taken into account by the overall heat transfer coefficient in the evaporator. Contrary to Kiranoudis and Markatos [1], who adopted a constant freezing point and a correspondent latent heat of chilling as shown by the dashed line in Fig. 3, in this work the apparent specific heat described by Chen [5] is used.

According to Chen's model, the apparent specific heat below the freezing point is given by the following equation:

$$c_{\text{apparent}} = 1.55 + 1.26x_s - \frac{(x_{w0} - x_b)L_0 t_f}{t^2}$$

where:

c_{apparent} = apparent specific heat, kJ kg^{-1} K^{-1}

x_s = mass fraction of solids

x_{w0} = mass fraction of water above the initial freezing point

x_b = mass fraction of bounded water

L_0 = latent heat of fusion of the water (= 333.6 kJ kg^{-1})

t_f = initial freezing point of food, °C

t = food temperature, °C

The integral form of this equation is shown by the continuous line in Fig. 3. It is apparent that this integral represents the enthalpy of the food as a function of temperature. Note that above the freezing point the specific heat of slabs, c_S, is taken constant, equal to c_{unfrozen}. The experimental values of the specific heats, for a wide range of foods, can be found in the open literature.

Considering the tunnel as a heat exchanger, the heat transfer and the temperature profile can be calculated from the following ordinary differential equation:

$$m \cdot c_S \cdot \mathrm{d}T = -(T - T_E) \cdot AU_E \cdot \mathrm{d}x \tag{1}$$

where:

x = relative position in the tunnel from the entrance to the exit [$= x/L$]

T = food temperature at position x

T_E = refrigerant saturated temperature at the evaporator

c_S = specific heat of the food

Therefore, the total refrigeration load can be expressed as:

$$Q_E = -\int_{T_0}^{T_{\text{out}}} m \cdot c_S(T) \cdot \mathrm{d}T \tag{2}$$

The total heat transferred by the condenser is given by:

$$Q_C = AU_C \cdot (T_C - T_0) \tag{3}$$

where:

T_C = saturated temperature of the refrigerant in the condenser

T_0 = temperature of the environment

It should be noted that the superheat of the refrigerant is not taken into account because it does not fundamentally change the dynamic behaviour of the system. For example, a desuperheating of 100 K is responsible of only 20% of the total heat rejected at the condenser, therefore the error introduced in the saturated temperature will be roughly of 2 or 3 K. It is obvious that in the case of refrigerants having a positive $\mathrm{d}s/\mathrm{d}T$ at the dew line, no error will be introduced.

Internal irreversibilities due to the refrigeration system are introduced. To that purpose, we keep the simplified approach given in Kiranoudis and Markatos [1], that allows the thermodynamic cycle and the compressor efficiencies to be determined. By considering an ideal refrigeration cycle including an adiabatic throttling process and considering an incompressible fluid, the following relations can be written:

$$Q_E = \left[\Delta h_R - c_R(T_C - T_E)\right] \cdot m_R \tag{4}$$

$$Q_C = \left[\Delta h_R \frac{T_C}{T_E} - c_R(T_C - T_E)\right] \cdot m_R \tag{5}$$

$$W_R = Q_C - Q_E = \Delta h_R \cdot m_R \frac{T_C - T_E}{T_E} \tag{6}$$

where:

Q_E = refrigeration load

Q_C = heat rejected at the condenser

W_R = work received by the refrigerant

c_R = mean specific heat of the refrigerant between T_C and T_E

Δh_R = refrigerant specific enthalpy of evaporation at T_E

m_R = refrigerant mass flow rate

In this model, the specific heat of the refrigerant, c_R, is assumed to be constant and, it is evaluated at the nominal operation point, while Δh_R is calculated as:

$$\Delta h_R = a + b \cdot \left(T_E - T_E^0\right) \tag{7}$$

T_E^0 is the evaporator temperature at the nominal operation point. The coefficients a and b are calculated from the tables. Even though, this relation gives a good level of realism, it should be pointed out that it is not suitable for all refrigerants and evaporation temperatures.

Introducing the compressor isentropic efficiency, η_R, the input electrical power is expressed by:

$$W = \frac{W_R}{\eta_R} \tag{8}$$

3. Cooling power intensification

Sorin and Rheault [6] have used the system exergy output to intensify chemical separation processes. They showed that the transfer of exergy can be explained as the product of the mass flow rate and an intensive quantity difference, which allows a very simple representation to be obtained. In this paper, the same method is applied for optimizing the cooling power in deep chilling tray tunnels.

The exergy balance around the general system shown in Fig. 4, yields:

$$W = \Delta E + D \tag{9}$$

Where W is the supplied power, ΔE is the rate of exergy increase associated with the mass flow rate, and D the rate of exergy destruction. Using the definition of exergy given by:

$$\Delta E = \Delta H - T_0 \Delta S \tag{10}$$

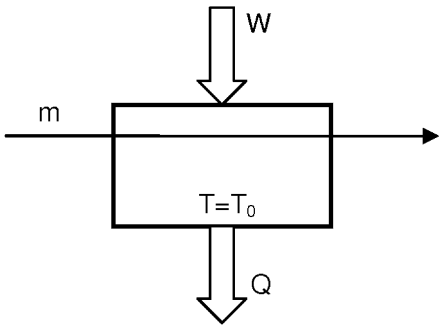

Fig. 4. Exergy balance model.

and considering a constant specific heat, c_S, yields:

$$\Delta E = c_S(T_0 - T_{\text{out}}) - T_0 \int_{T_{\text{out}}}^{T_0} c_S \frac{\mathrm{d}T}{T}$$

$$\Delta E = -c_S(T_{\text{out}} - T_0) + T_0 c_S \ln\left(\frac{T_{\text{out}}}{T_0}\right)$$

$$\Delta E = -Q_E\left(1 - \frac{T_0}{\widetilde{T}}\right) \tag{11}$$

where:

$$Q_E = c_S(T_{\text{out}} - T_0)$$

$$\widetilde{T} = \frac{T_{\text{out}} - T_0}{\ln(\frac{T_{\text{out}}}{T_0})} \tag{12}$$

According to Eq. (11), the change in exergy can be written as the product of the refrigeration load (Q_E) and an equivalent temperature potential $\tilde{\theta} = (1 - T_0/\widetilde{T})$, thus:

$$\Delta E = -Q_E \tilde{\theta} \tag{13}$$

In general, the evaluation of exergy destruction, D, must include various losses and non-linearities that will be in detrimental of the comprehension of more essential exergy transfers. A more detailed analysis of the numerical simulation will be discussed in the following sections; thus, herein an ideal refrigeration system that rejects heat at a temperature T_C above the environmental temperature T_0, is assumed. Therefore, the only irreversibilities are the heat transfer taking place at the evaporator and at the condenser, respectively. Under these conditions, the exergy balance around an ideal heat pump can be written as:

$$Q_C \theta_C = Q_E \theta_E + W \tag{14}$$

Using the first law of thermodynamics yields:

$$(Q_E + W)\theta_C = Q_E \theta_E + W$$

$$Q_E(\theta_C - \theta_E) = W(1 - \theta_C) \tag{15}$$

In addition, Eq. (9) can be rewritten more explicitly as:

$$\Delta E_{\text{exp}} = P + D \tag{16}$$

where, ΔE_{exp} represents the rate of exergy expenditure and P the exergy power associated with cold production. Further, using Eqs. (13) and (15), the destruction of exergy power is written as:

$$D = Q_E(\tilde{\theta} - \theta_E) + (Q_E + W)\theta_C \tag{17}$$

This equation allows the exergy transfer to be summed up on a simple graphical representation, as shown in Fig. 5.

Since Q_E is a monotone increasing function of $(\tilde{\theta} - \theta_E)$, it can be clearly seen from this figure that for a constant θ_E there exists a value of $\tilde{\theta}$ for which P reaches a maximum. Moreover, it can be also observed that this maximum does not depend on the dimensions of the system but rather on the temperatures. Although most of the optimization techniques consist of finding a maximum energy efficiency for a given exergy expenditure, i.e., by changing the allocation of system dimensions, instead

Table 1
Moisture content, protein content, initial freezing point, and specific heats of beef steak [5]

Beef	Moisture content, % x_{w0}	Protein, % x_p	Bound water, % x_b	Initial freezing point, °C	Specific heat above freezing, kJ kg^{-1} K^{-1}	Specific heat below freezing, kJ kg^{-1} K^{-1}	Latent heat of fusion, kJ kg^{-1}
Round, full cut, lean	70.83	22.03	$x_b \approx 0.4x_p$	−1.7	3.52	2.12	237

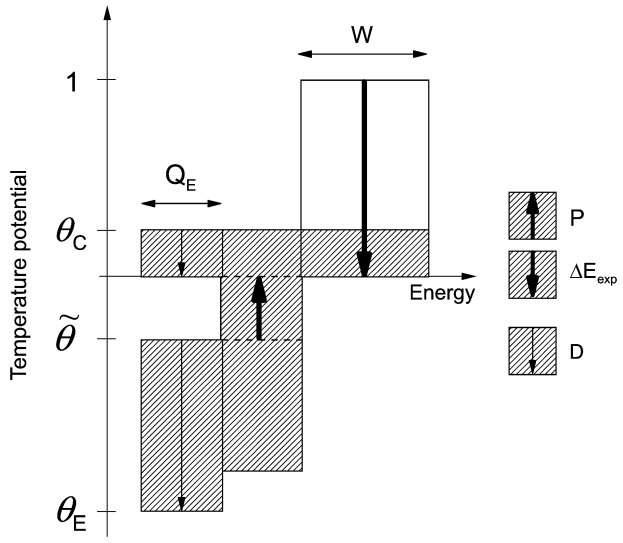

Fig. 5. Graphical representation of the exergy transfer.

this work looks for the maximum exergy production (i.e., by changing the system operation variables), together with the associated destruction of specific exergy, a useful efficiency-like indicator to be determined when the process output is a product. The destruction of specific exergy is defined as:

$$d = \frac{D}{m} \tag{18}$$

Due to conduction heat transfer, both Q_E and θ_C increases with increasing $\tilde{\theta}$ (see Fig. 5). Thus, the exergy power destruction results in a monotone increasing function of $(\tilde{\theta} - \theta_E)$, i.e., the mass flow rate. However, for an infinite mass flow rate, the exergy power destruction will reach a maximum with $\tilde{\theta}$ equal to zero (i.e., the output temperature becomes equals to the input temperature). As a consequence the exergy power destruction per unit of mass tends to cancel. Taking into account that the exergy power destruction flattens out when the production falls, the destruction of specific exergy passes through a maximum at a given production rate. It is obvious that the destruction of specific exergy stands for the generation of irreversibilities per unit of the mass product and represents the effort spent per unit of mass by a finite-time process.

4. A studied case

Kiranoudis and Markatos [1] presented the optimal design of a 1100 kg s^{-1} capacity tray tunnel handling meat 2 kg kg^{-1} db wet. Under this condition, the refrigerant temperature was −32.7 °C at the evaporator and 32.6 °C at the condenser. The inlet temperature of the meat was 20 °C and the targeted output

Table 2
Thermophysical properties of ammonia

Ammonia	Heat capacity of liquid phase	Latent heat of vaporization
Formula	$c_R = 0.5 \cdot (c_p(T_C^0) + c_p(T_E^0))$	$\Delta h_R = a + b(T_E - T_E^0)$
Parameters	$T_C^0 = 32.6\,°C$, $T_E^0 = -32.7\,°C$	
Results	$c_R \approx 4.652$ kJ kg^{-1} K^{-1}	$a \approx 1368$ kJ kg^{-1} $b \approx -2.974$ kJ kg^{-1} K^{-1}

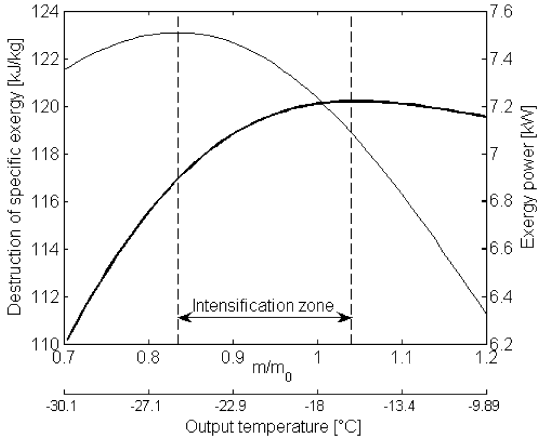

Fig. 6. Exergy power and destruction of specific exergy as a function of relative food mass flow rate.

temperature was −18 °C. The data presented by the authors are quite useful because the knowledge of the meat and the refrigerant properties can be used to estimate the value of the overall heat transfer coefficients AU_E and AU_C at the evaporator and the condenser respectively. In addition, in the present work the same compressor efficiency, i.e., 70%, as that reported by Kiranoudis and Markatos is used. Furthermore, the meat properties [5] are reproduced in Table 1: It is assumed that ammonia is used as the refrigerant fluid having the thermophysical properties at nominal operation point listed in Table 2: For a given evaporator temperature T_E equal to the design value, the mass flow, m, is changed (i.e., the output temperature, T_{out}) in order to maximize the cooling power P and to minimize the destruction of specific exergy d. At the nominal evaporator temperature of −32.7 °C, the results are shown in Fig. 6 as a function of the relative mass flux, i.e., the ratio between the actual flow rate and the initial flow rate (m/m_0). For each mass flow rate, the corresponding output temperature is also shown along the axis.

This figure shows the existence of two maximums, one for the exergy power and the second for the destruction of specific exergy. These maximums can be used to identify three

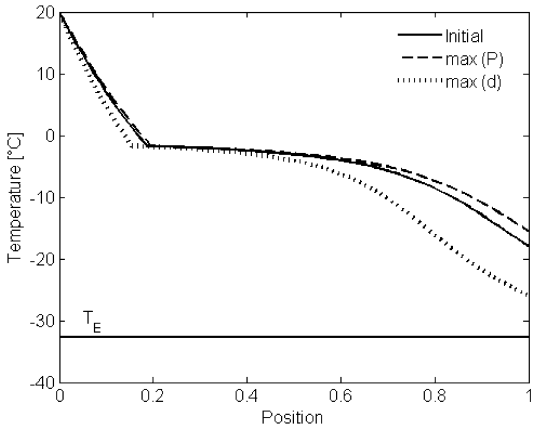

Fig. 7. Food temperature profiles in the tunnel.

different regions. The region located between the two bounds is important because here, the exergy power increases with decreasing the specific exergy, which corresponds to an increase of the objective function. It is obvious that the system should be optimized in this region, called the intensification region. Further, within the regions located at the left and the right sides of the figure, both indicators (d and P) have opposed effects. This means that when the exergy power increases (positive effect), the destruction of specific exergy increases (negative effect) and vise versa. Thus, no optimization can be carried out within these regions. It is important to remark that in the intensification zone, the trade off between high mass flow rate (quantity) and low output temperature (quality) depends on the operational requirements. Moreover, it must be pointed out that the maximum of the destruction of specific exergy, shown in Fig. 6, is not systematic; it depends on the internal and external irreversibilities of the refrigeration system and on the variation of the specific heat with temperature.

By assuming that the system operates under nominal conditions and the quantity must be intensified then, it is observed that the exergy power increases (shift toward the right side of Fig. 6). This exergy power represents a compromise between the quantity and the quality. When this compromise reaches its maximum, the food mass flow rate should not be increased any more; from this point the exergy power starts decreasing. Thus, the maximum of exergy power represents a limit for quantity intensification. In turn, assuming the same operation conditions and assuming that the quality must be intensified then, the food mass flow rate must be decreased in order to obtain a decrease in the output temperature. Moreover, a quality intensification produces a shift towards the left side of Fig. 6 where the destruction of specific exergy increases. Since the destruction of specific exergy represents losses, this maximum should be avoided. It is obvious that this maximum represents a limit to quality intensification.

For mass flow rates corresponding to the two extremities of the intensification interval, it is possible to determine the output temperature of the food. To this purpose, for each specific food mass flow rate, a temperature profile must be calculated along the tray tunnel. These profiles are shown in Fig. 7. The higher temperature profile corresponds to the maximum cold

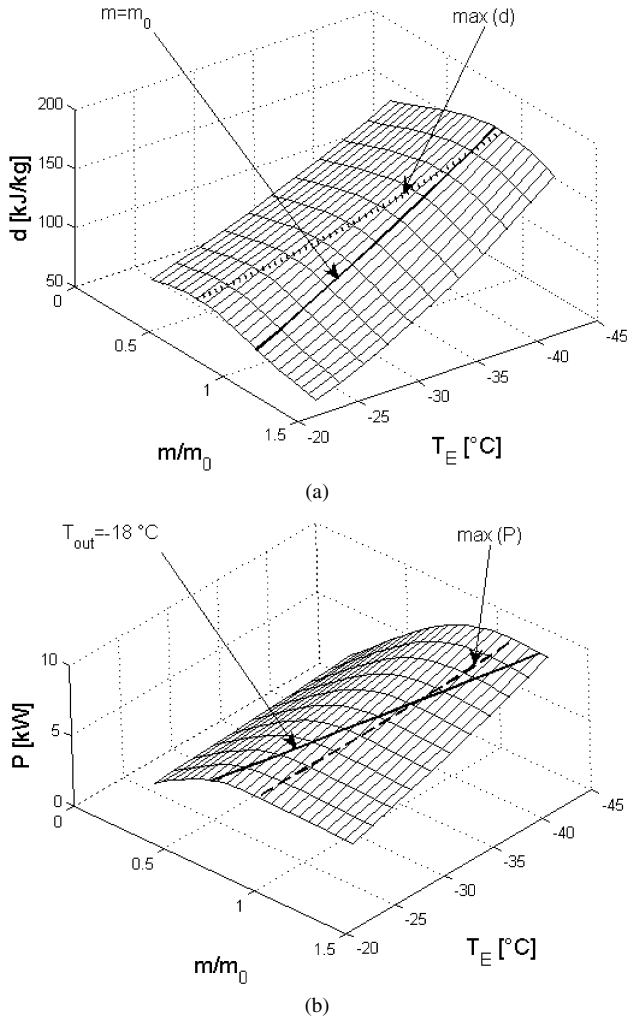

Fig. 8. Optimization surfaces. (a) Destruction of specific exergy. (b) Exergy power.

production while the lowest one, corresponds to the maximum destruction of specific exergy.

Further, if the evaporator temperature is allowed to change then, the representation of the problem becomes three-dimensional. In this new representation, the first independent variable is the food mass flow rate that is linked with the temperature level, the second independent variable is the evaporator temperature while the optimization functions are P or d. The resulting 3D surfaces are shown in Fig. 8. These surfaces represent extruded images of the curves plotted in Fig. 6 as a function of the evaporator temperature T_E, as if a series of Fig. 6 was generated for different evaporator temperature. Since, in reality, the food output temperature is not supposed to change because it must fulfill specified sanitary reasons, the introduction of a new optimization variable, i.e., the evaporator temperature, gives way to the following analysis.

For each evaporator temperature, a mass flow rate exists for which the output food temperature matches the desired target ($-18\,^{\circ}\mathrm{C}$ for the present case). The line corresponding to this temperature is shown in Fig. 8(b). In the same manner, we could hypothetically operate the system at a constant mass flow rate and let the output temperature to change. This particular case

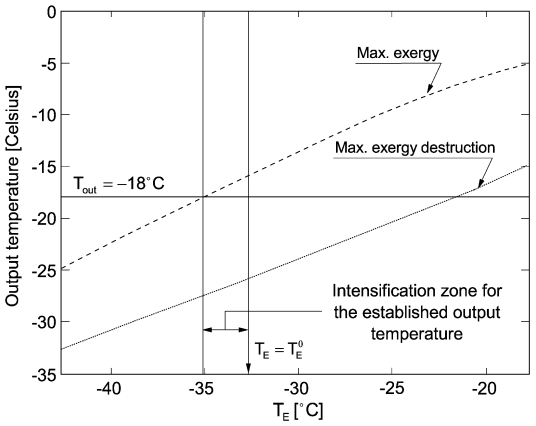

Fig. 9. Bounds of the output food temperature as a function of evaporator temperature.

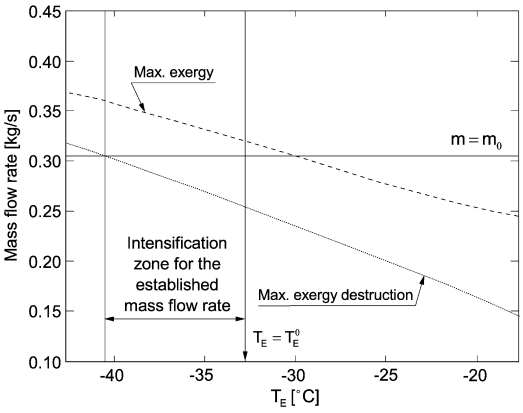

Fig. 10. Bounds of food mass flow rates as a function of evaporator temperature.

is also represented in Fig. 8(a). It can be observed from these 3D surfaces, and in particular along these two particular lines, that no absolute throughput intensification is possible since both the exergy power and the specific exergy destruction increase continuously with decreasing the evaporator temperature, T_E. However, new indexes that represent the relative exergy power and the relative destruction of specific exergy can be defined. At a given evaporator temperature, they are respectively the actual exergy power divided by the maximum possible exergy power and the actual destruction of specific exergy divided by the local maximum of specific exergy destruction. Thus, the performance of the actual process is compared with that of an unconstrained system where the food mass flow or the food output temperature are variables.

In Fig. 9, the food output temperature corresponding to the maximums of these indicators is plotted as a function of the evaporator temperature. The band delimitated by these two lines is the intensification zone defined above. Now, for a given output temperature (the horizontal line on Fig. 9), it can be observed that two evaporator temperatures exist for which, the given output temperature corresponds either to the local maximum of exergy power (at the left) or to the local maximum of the destruction of specific exergy (at the right). To keep the output temperature constant, the evaporator temperature must be decreased when the mass flow rate is intensified. As a consequence, in order to intensify the quantity, the evaporator temperature must be lower than its nominal value. However, the evaporator temperature should not drop beyond a certain limit. This limit is encountered when the food mass flow rate corresponds to the local maximum of exergy power. Below this limit, the exergy power goes below the local maximum. As a consequence, an intensification zone can be defined for the evaporator temperature when the output temperature is constant.

Fig. 10, represents a view of Fig. 8 in the m–T_E plan. In the same manner, the two mass flow rates corresponding to the above defined intensification bounds are plotted as a function of the evaporator temperature. The fixed mass flow rate crosses these lines at two particular points that define two specific evaporator temperatures. These special cases are encountered either when the fixed mass flow rate corresponds to the local maximum of specific exergy destruction (at the left) or when the fixed mass flow rate corresponds to the local maximum of exergy power (at the right). If the food mass flow rate is constant then, the evaporator temperature must be lower than the food output temperature. Thus, in order to intensify the quality, the evaporator temperature must be lower than its nominal operation value. However, the evaporator temperature should not approach a given limit where the food mass flow rate corresponds to the local maximum of specific exergy destruction. Fig. 10 shows the intensification zone for a constant mass flow rate thereof.

5. Conclusions

This paper shows that the intensification of chilled food production is not a straightforward process due to the fact that not only the food mass flow rate should be considered but also the level of the output food temperature. From this analysis the following question arises: is it better to have a high mass production at high food temperatures, or rather reduce the mass production but reaching lower output food temperatures? As an answer to this important question, an indicator was found that represents a compromise between quantity and quality: exergy, since it is the product of the extracted heat (Q_E) and the Carnot function ($\tilde{\theta}$).

The destruction of specific exergy, in addition to the exergy power, was proved to give useful information on the system behaviour. Depending upon the priority, i.e., quality or quantity, the operator is able to select an operating mode within well-specified limits.

When the food mass flow rate or output temperature is constrained, it has been shown that an intensification zone could be defined, provided that the evaporator temperature was considered as an optimization variable

In order to carry out this analysis, we ignored the limitation that normally applies to the food output temperature due to sanitary constraints. In addition, the numeric calculations did not include the compressor capacity and temperature limitations. It must be pointed out that the final optimization of a food deep chilling tray tunnel will depend on factors such as economic and

schedule constraints, which were not considered in the present study.

Acknowledgements

This work was funded by the discovery grant RGPIN 41929 of the Natural Sciences and Engineering Research Council of Canada (NSERC).

References

[1] C.T. Kiranoudis, N.C. Markatos, Design of tray tunnels for food deep chilling, Journal of Food Engineering 40 (1999) 35–46.

[2] A. Bejan, Entropy generation minimization: The new thermodynamics of finite-size devices and finite-time processes, Journal of Applied Physics 79 (3) (1996) 1191–1218.

[3] V.M. Brodyansky, M.V. Sorin, P. Le Goff, The Efficiency of Industrial Processes: Exergy Analysis and Optimization, Elsevier, Amsterdam, 1994.

[4] M. Sorin, F. Rheault, B. Spinner, On exergy destruction and maximum power output in heat engines, in: 18th International Congress of Mechanical Engineering, 6–11 November 2005, Ouro Preto, Minas Gerais, Brazil, COBEM 2005, CD-ROM.

[5] Thermal properties of foods, 2002 ASHRAE Refrigeration Handbook, ASHRAE, pp. 8.1–8.9.

[6] M. Sorin, F. Rheault, Thermodynamically guided intensification of separation processes, in: 8th Conference on Process Integration, Modelling and Optimisation for Energy Saving and Pollution Reduction, 2005, pp. 19–24.